Recent recovery of the Siberian High intensity

Jee-Hoon Jeong,[1] Tinghai Ou,[1,2] Hans W. Linderholm,[1] Baek-Min Kim,[3] Seong-Joong Kim,[3] Jong-Seong Kug,[4] and Deliang Chen[1]

Received 3 March 2011; revised 6 September 2011; accepted 30 September 2011; published 2 December 2011.

[1] This study highlights the fast recovery of the wintertime Siberian High intensity (SHI) over the last two decades. The SHI showed a marked weakening trend from the 1970s to 1980s, leading to unprecedented low SHI in the early 1990s according to most observational data sets. This salient declining SHI trend, however, was sharply replaced by a fast recovery over the last two decades. Since the declining SHI trend has been considered as one of the plausible consequences of climate warming, the recent SHI recovery seemingly contradicts the continuous progression of climate warming in the Northern Hemisphere. We suggest that alleviated surface warming and decreased atmospheric stability in the central Siberia region, associated with an increase in Eurasian snow cover, in the recent two decades contributed to this rather unexpected SHI recovery. The prominent SHI change, however, is not reproduced by general circulation model (GCM) simulations used in the IPCC AR4. The GCMs indicate the steady weakening of the SHI for the entire 21st century, which is found to be associated with a decreasing Eurasian snow cover in the simulations. An improvement in predicting the future climate change in regional scale is desirable.

Citation: Jeong, J.-H., T. Ou, H. W. Linderholm, B.-M. Kim, S.-J. Kim, J.-S. Kug, and D. Chen (2011), Recent recovery of the Siberian High intensity, *J. Geophys. Res.*, *116*, D23102, doi:10.1029/2011JD015904.

1. Introduction

[2] The Siberian High (SH) is the most conspicuous pressure system found in the Northern Hemisphere during wintertime. Strong radiative cooling over the snow covered Eurasian continent forms a cold-core high-pressure system in the lower troposphere over northern Mongolia, which exhibits the temporal and spatial variability of substantial amplitude exerting tremendous influences on weather and climate in Northern Eurasia, East Asia, and even further into South Asia [e.g., *Cohen et al.*, 2001; *Panagiotopoulos et al.*, 2005; *Wang*, 2006]. On synoptic to intraseasonal time-scales, the strengthening and east-southward expansion of the SH directly results in severe cold-surge outbreaks in East Asia often accompanied by heavy snowfall events [*Boyle and Chen*, 1987; *Zhang et al.*, 1997]. On the interannual to interdecadal time-scales, the SH intensity (SHI) is a primary factor in determining the strength of the East Asian Winter Monsoon (EAWM) circulation. The pressure difference between the SH and the Aleutian low in the North Pacific causes strong northwesterly winds, yielding a steep meridional temperature gradient along the East Asian coastal region, which characterizes the EAWM circulation [*Chang et al.*, 2006]. Together with the Arctic Oscillation (AO) [*Thompson and Wallace*, 1998], the SHI can account for more than half of the interannual variability of winter mean temperature in East Asia [*Gong and Ho*, 2002]. Therefore, the accurate prediction of SHI is one of the essential factors for weather and climate prediction in the vast area of the Eurasian continent.

[3] Several observational studies previously reported a significant weakening of the SHI during the second half of the 20th century [e.g., *Gong and Ho*, 2002; *Panagiotopoulos et al.*, 2005; *Sahsamanoglou et al.*, 1991]. The most striking feature found in the observations was the "dramatic" decreasing SHI trend of 2.5 hPa/decade for the period 1978–2001 in the work by *Panagiotopoulos et al.* [2005]. Although the underlying dynamical causes have not been explicitly addressed, the weakening of the SHI has been generally considered as a plausible consequence of climate warming because the long-term variation of the SHI showed a high negative correlation with that of surface temperature over the northern Eurasian region [*D'Arrigo et al.*, 2005; *Gong and Ho*, 2002; *Panagiotopoulos et al.*, 2005]. In addition to observational evidence, simulations from global climate models (GCMs) supported this assumption in that the general response of GCMs to increasing greenhouse gas (GHG) concentrations was a decline in sea level pressure (SLP) over northern Eurasia accompanied by surface warming [*Gillett et al.*, 2003; *Liu et al.*, 2009].

[4] In contrast to the general perception of the declining SHI under climate warming conditions, here we present a

[1]Department of Earth Sciences, University of Gothenburg, Gothenburg, Sweden.
[2]School of Geography, Beijing Normal University, Beijing, China.
[3]Korea Polar Research Institute, Incheon, South Korea.
[4]Korea Ocean Research and Development Institute, Ansan, South Korea.

0148-0227/11/2011JD015904

very fast strengthening trend of the winter SHI over the last two decades by analyzing various observational data sets. Recent changes in Eurasian snow cover and surface air temperature (SAT) trend are suggested as possible causes for this distinct, but rather an unexpected change. Further, the SHI for the 20th and 21st centuries simulated by GCMs used in the Fourth Assessment Report of the Intergovernmental Panel on Climate Change (IPCC AR4) [*Intergovernmental Panel on Climate Change*, 2007] are examined.

2. Utilized Data

[5] The SHI is defined as the winter (December to February) mean SLP over northern Mongolia between 40 and 65°N and 80–120°E (the central SH region hereafter), where the maximum SH SLP center is found in winter. The same or similar definitions of the SHI have been utilized in many previous studies [e.g., *Gong and Ho*, 2002; *Panagiotopoulos et al.*, 2005; *Wu and Wang*, 2002]. The time series of SHI are derived from i) two observational gridded data sets: the Hadley Centre SLP (HadSLP2) [*Allan and Ansell*, 2006] and the National Centre for Atmospheric Research SLP (NCARSLP) [*Trenberth and Paolino*, 1980]; ii) two reanalysis data sets: NCEP/NCAR (NCEP) [*Kalnay et al.*, 1996] and ERA40 (ERA40) [*Uppala et al.*, 2005]; and iii) and in situ SLP observations from 20 stations located in the central SH region, the same stations used by *Panagiotopoulos et al.* [2005]), complied by NCAR (available at http://dss.ucar.edu/datasets/ds570.0/. Additionally, to examine the temporal SHI variation on multidecadal time-scales, a reconstruction of the SHI based on Eurasian and North American tree rings from *D'Arrigo et al.* [2005], spanning from 1599 to 1980, is used. Although this reconstruction only reflects part of the SHI variance (42% based on the statistical association between the tree ring data and instrumental observations during the overlapping calibration period), and that, in general, tree ring reconstructions are known to have large uncertainties in resolving long-term (centennial and longer) variability due to the requisite detrending processes [*Esper et al.*, 2002], the reconstructed temporal SHI variation on interdecadal time-scales fairly well matches the 20th-century observations (see Figure 1b) [*D'Arrigo et al.*, 2005].

[6] To investigate the possible mechanism behind the observed SHI change, we examine changes in SAT, snow cover, and tropospheric air temperature from observations and reanalysis data sets. A gridded data set of global historical land surface temperature anomalies provided by the Climatic Research Unit at the University of East Anglia (CRUTEMP3) [*Brohan et al.*, 2006] is utilized for the SAT. For snow cover, two data sets provided by the National Snow and Ice Data Center (NSIDC) [*Armstrong and Brodzik*, 2005] and Global Snow Lab (GSL) at Rutgers University [*Robinson et al.*, 1993] are used. For the tropospheric air temperature, four reanalysis data sets: NCEP, NCEP/DOE (NCEP II) [*Kanamitsu et al.*, 2002], ERA-40 [*Uppala et al.*, 2005], ERA-interim [*Dee and Uppala*, 2009] and the Japanese 25-year reanalysis (JRA25) [*Onogi et al.*, 2007] are utilized.

[7] The present study also examines the changes in the SHI and associated variables: snow cover, SAT, and atmospheric stability simulated by GCMs for the 20th and 21st century. The 20C3M and SRESA1b simulations from 22 GCMs used for the IPCC AR4 are synthesized. All data are taken from the World Climate Research Programme's (WCRP's) Coupled Model Intercomparison Project phase 3 (CMIP3) multimodel data set [*Meehl et al.*, 2007] (data available at http://www-pcmdi.llnl.gov/ipcc/about_ipcc.php with full names and details of 22 GCMs). When defining the SHI with the GCM simulations, the central SH region is defined with the same areal box used for observational SLP (40–65°N and 80–120°E). This is because, although every GCM has a systematic bias of SLP to some degree, overall features of SH in its extent and central location are found to be relatively well capture by majority of GCMs.

3. Results

3.1. Observed Variation of SHI

[8] Figure 1 presents the time series of the SHI from the 17th century to the present (note that each of the time series is normalized based on its mean and standard deviation for the period 1958–1980, the common period for all observational SLP data sets used). The most conspicuous feature during the 20th century (Figure 1a) is a steep declining SHI trend from the 1970s to 1990s leading to record-low SHIs for most observational data sets in the early 1990s. Only the NCEP reanalysis data set shows a very weak trend during this period, but this is likely associated with the known systematic bias of the NCEP reanalysis in representing interdecadal changes over the Eurasian continent [*Wu et al.*, 2005], leading to an exaggerated cold period around 1972–1977 compared to other data sets. In the early to mid 1990s, however, the declining trend sharply turned to positive, and the SHI records shows a continuous recovery, reaching the climatologically normal state in recent years. The rate of this recent recovery appears to be slightly faster than that of the preceding decline, and different data sets show similar magnitudes of the positive trend despite the large amplitude of interannual variability in recent decades. The NCARSLP has a slightly different trend change showing a more continuous decline of the SHI until the mid-1990s. However, also here a recovering trend is evident in recent years albeit less pronounced compared to the other ones. The long-term evolution of SHI found from the tree ring reconstruction (Figure 1b) indicates that the SHI underwent about a dozen of distinct interdecadal fluctuations during the last four centuries. Despite limitations in tree ring reconstruction, the amplitude of the recent interdecadal SHI variation seems to exceed that of any interdecadal SHI variation found from the 17th to the early 20th centuries. Also, *D'Arrigo et al.* [2005] pointed out that the decline of the SH after 1980 is the largest shift during the interval covered by their SHI reconstruction.

3.2. Associated SAT and Eurasian Snow Cover Changes

[9] Since the change in SAT in the SH region and the associated change in surface radiation directly affects the strength of the SH [*Ding*, 1990], the Northern Hemisphere or global warming in the second half of the 20th century could be regarded as a plausible cause of the declining SHI. However, the steep recovery of the SHI in the recent two decades seems to be inconsistent with the continuous progression of the Northern Hemispheric or global scale warming. Therefore, we presume that some localized climate feedback working

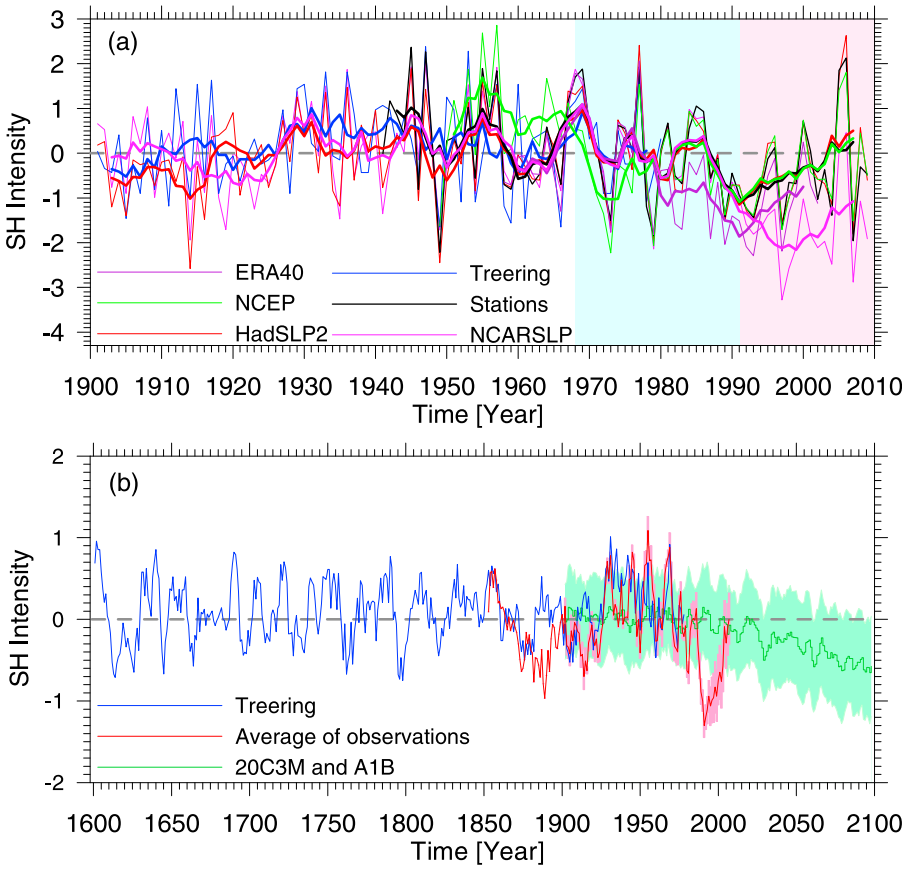

Figure 1. (a) Time series of winter (DJF) SHI derived from 5 SLP data sets from 1900 to 2009. Thick lines indicate 5-year running averaged time series. Each time series is standardized for the comparison with respect to the mean and standard deviation for 1958–1980 of each data set. The area with a background color of sky blue (pink) indicates the period of SHI decline (incline) defined in the present study. (b) Comparison of the winter SHI time series reconstructed from tree rings, the average of 5 SHI time series from observational SLP data sets (each data set is standardized before taking the average) from the 17th century to present, and simulated and projected SHI by the CMIP3 experiments for the 20th and 21st century under 20C3M and A1B scenarios, respectively. The pink envelope around the average SHI from observations indicates 1 standard deviation of between-data set differences. The thick green line indicates the ensemble averaged SHI of 22 GCMs, and 1 standard deviation of between-model differences is indicated by the light green envelope. The SHI from each model is standardized (also based on the mean and standard deviation for 1958–1980) before taking the ensemble average. For brevity of the figure, 5-year moving averaged time series are shown.

against the long-term tendency of Northern Hemisphere or global warming might have contributed to the recent change in the SHI. By examining more localized changes, it indeed is found that the winter SAT in the central SH region underwent a remarkable trend change in the early 1990s. From Figure 2a, it is clearly seen that the SH central region SAT exhibited very similar temporal variations as the global and Northern Hemispheric SAT averages before the early 1990s, displaying a large surface warming trend from the 1970s to 1990s. However, subsequently the SH central region SAT trend began to diverge from the both large-scale SAT trends, instead displaying rather a slightly negative trend accompanied by large interannual variability. *Cohen et al.* [2009] also found a similar decreasing trend in the late winter (January to March) Eurasian SAT for 1989–2008 contrasting to vigorous warming in late autumn to early winter (October to December).

[10] This distinct trend change in SAT in the SH central region after the early 1990s seems to be contributed by the climate feedback effect associated with an increase in Eurasian snow cover. Figure 2b shows the time series of snow cover extent (SCE) over northern Eurasia (30–70°N, 55–135°E) in late fall (October to November) and winter (December to January) from the mid-1960s to present. Despite very large interannual variability before the 1980s (before the era of satellite observation), the late fall Eurasian SCE shows a decreasing trend until the early 1990s, roughly displaying the opposite tendency as the winter SAT in the SH central region does. Interestingly, this declining trend turned positive in the early 1990s, seemingly coinciding with commencing of the cooling trend in the SH central region. The winter SCE also showed a clear decreasing trend in the 1970s, but no obvious trend is evident from the mid-1980s to the mid-1990s unlike

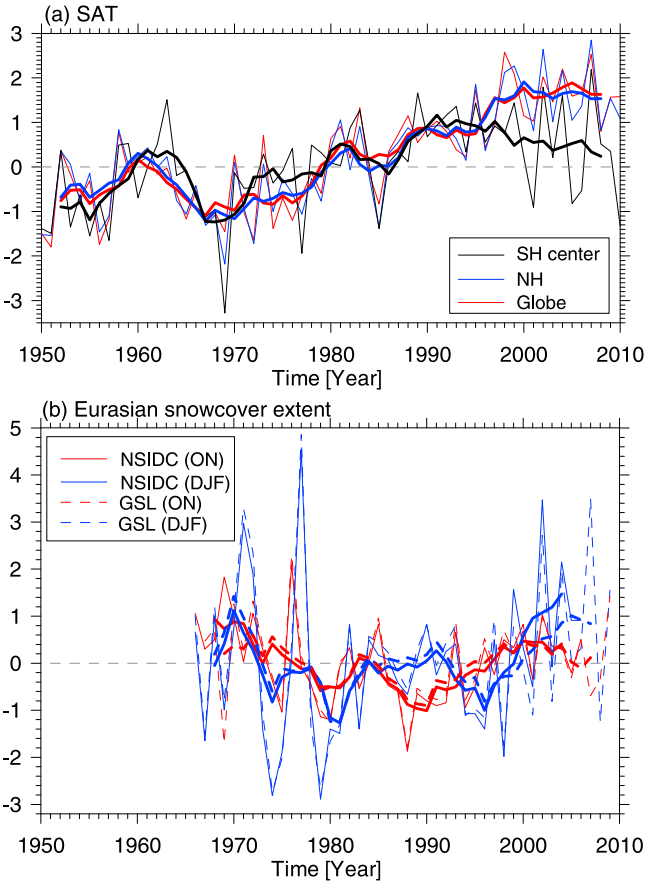

Figure 2. Time series of (a) SAT averaged over the central SH region, Northern Hemisphere, and globe and (b) Eurasian snow cover extent in winter (DJF) and late fall (ON). Each time series is standardized for comparison. Thick lines indicate 5-year running averaged time series.

that of the late fall SCE. But the increasing trend is also evident from the late 1990s.

[11] The coherent change between SAT in the SH center and Eurasian snow cover in recent decades may relate to the snow-albedo feedback relationship, where the warming (cooling) melts more (less) snow which again feeds warming (cooling) by reflecting less (more) incident solar radiation. Consequently, the alleviated SAT warming trend in the central SH region after the early 1990s could be an effect of the increasing SCE trend. This coherent tendency is more clearly seen from the late fall SCE and winter SAT. This is perhaps because the change in SCE and SAT in winter may be less sensitive with each other over the northern Eurasian continent where SAT is well below −10 degree and surface is mostly snow covered more than 90% (figure not shown), so local warming (or cooling) is not much influential on snow melting or freezing. Instead, a lagged influence of late fall SCE on SAT in the following winter is considered to be a primary mechanism to invoke the feedback effect. A possible mechanism can be proposed as follows: as the surface cold-core of the SH begins to develop in late fall, the anomalous high (low) SCE in late fall reinforces an early build-up of cold (relatively warm) surface air masses, due to its slowly varying characteristics with respect to the overlying atmosphere, which leads to an anomalous high (low) SHI in the following winter. To test this physical link, correlations between the local snow cover anomalies in late fall and SAT in late fall and following winter are analyzed (Figure 3). All data sets are high-pass (<5 years) filtered before calculating correlations in order to exclude correlations from long-term trend. Overall, results well support the suggested lagged relationship between the Eurasian SCE and SAT. Over most of northern Eurasia, local SAT and snow cover in late fall are negatively correlated for both periods of decreasing and increasing SHI (Figures 3a and 3b). Despite the lower significance and amplitude, SAT in the following winter well preserves the overall negative correlation with late fall snow cover (Figures 3c and 3d). Examining the spatial linear trend pattern of October to November SCE for 1967–1990 and 1991–2009 (Figures 3e and 3f), significant negative and positive trends in SCE are largely found over the mid-eastern Eurasian continent where the negatively correlated relationship between the winter SAT and late fall SCE is dominant. Considering that the negative correlation between SAT and snow cover remains almost unchanged throughout the period of the distinct SHI change, it can be concluded that both the warming and cooling trend in the SAT for the periods of decreasing and increasing SHI are contributed by the snow cover change.

[12] The air temperature change near the surface directly influences the surface pressure (i.e., the SHI) by affecting the 'air density'. In addition, large near surface temperature changes, being amplified by the snow-albedo feedback, could further modulate the SHI by altering the atmospheric vertical stability. For instance, the lower tropospheric atmosphere in the SH region, which is very stably stratified during winter, becomes less stable if a substantial warming occurs at near surface. Under these conditions, turbulent vertical mixing of heat and momentum can be enhanced. Consequently the steady build-up of cold and dense near-surface air can be hindered, and this can eventually weaken the surface high pressure. This seems to apply to the observed changes in the central SH region during the declining SHI phase (1970s to early 90s), while the opposite process seems to have operated during the recent SHI recovery. The vertical profiles of temperature trends in the SH center from reanalysis data sets (Figure 4a) display that the atmosphere warming and cooling rates are largest near the surface both before and after the early 1990s respectively. Although the long-term behavior of reanalysis data remain less reliable, especially for the high-latitudes and Arctic region [*Jones et al.*, 2011; *Wu et al.*, 2005], different reanalysis data sets are in good agreement with the vertical structure of the warming. The actual vertical temperature profiles for the periods 1989–1993 and 2005–2009, representing the period of lowest level of SHI and recent years of recovered SHI, indicate that the relatively strong near-surface cooling in recent two decades have led to increased atmospheric stability in the lower troposphere (below 700 hPa) over the SH region.

[13] So far in the present study, only the local feedback effect of snow cover change on SAT and SHI have been considered. However, many previous studies suggested that the Eurasian snow cover has sufficient potential to alter the large-scale atmospheric circulation in the following winter, which affects the SLP over a vast area of northern Eurasia and Arctic, including the SH region [*Cohen and Entekhabi*,

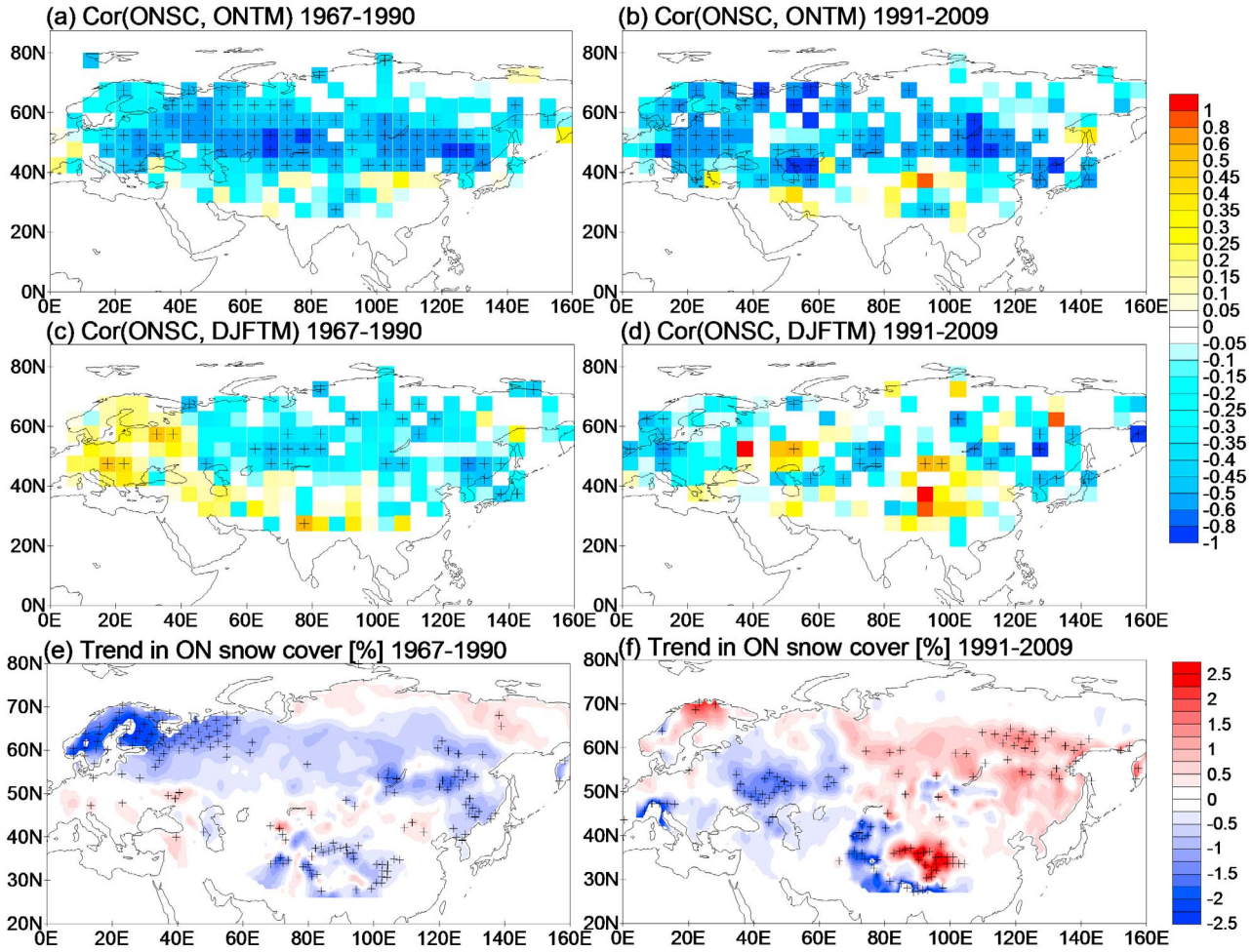

Figure 3. Correlation coefficients between SAT for October–November and GSL snow cover concentration for (a and c) October–November and (b and d) December–January. SAT and snow cover data sets are high-pass (<5 years) filtered before calculating correlation coefficients. (e and f) Trend in the GSL snow cover concentration for October–November. Figures 3a, 3c, and 3e are calculated with data for 1967–1990 and Figures 3b, 3d, and 3f are calculated with data for 1990–2009. Regions of correlation coefficient or trend significant over the 95% confidence level are indicated by crosses.

1999; *Cohen et al.*, 2007; *Fletcher et al.*, 2009; *Orsolini and Kvamstø*, 2009; *Saito et al.*, 2001]. Actually *Cohen et al.* [2001, 2007] also suggested a coherence between the anomalous high (low) Eurasian snow cover in late autumn and anomalous high (low) SH strength in the following winter, which is consistent with our findings. In particular, *Cohen et al.* [2007] introduced a possible dynamical model explaining the remote and delayed response of large-scale atmospheric circulation to snow cover change, which can be summarized as follows. If there is above normal Siberian snow cover in late autumn, diabatic cooling locally induces higher SLP anomalies (a strengthening of SH) and colder temperature. This promotes upward propagation of planetary waves to the stratosphere, which weakens stratospheric polar vortex in the following winter. Finally, downward propagation of associated geopotential height and wind anomalies to surface can induces negative AO in the troposphere, a weakening of tropospheric westerlies and colder temperature over the northern Eurasian continent. In addition to the observational analysis, such large-scale atmospheric response to the anomalous Eurasian snow cover in autumn is supported by numerical model simulations [*Cohen and Fletcher*, 2007; *Orsolini and Kvamstø*, 2009; *Saito et al.*, 2001]. *Cohen et al.* [2010] suggested the record low AO index observed in the winter of 2009–2010 resulted from the suggested coupling mechanism between the Eurasian snow cover and atmospheric circulations.

[14] Therefore, it is plausible that the large-scale circulation change, or AO, invoked by the Eurasian snow cover reinforced the strengthening (weakening) of SHI for the period of increasing (decreasing) snow cover in addition to the local feedback effect. Figure 5 suggests that a prominent change in the long term trend of the AO in recent decades has a relevance to the SHI change. The AO index and SHI exhibit a statistically significant negative correlation for the last 55 years (linear correlation coefficient is −0.37 for 1950–2004, >99% significance), which can be easily expected from the overlapping spatial extent of SLP signatures of the

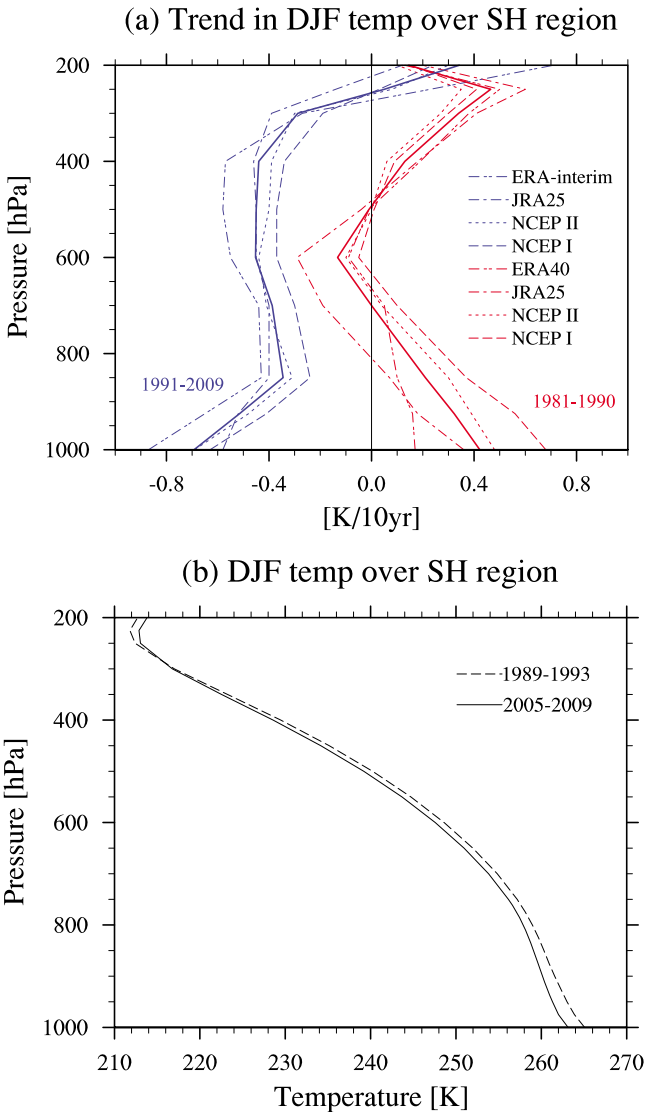

Figure 4. (a) Trends in winter mean air temperature averaged over the SH region from reanalysis data sets for the periods 1981–1990 and 1991–2009. (b) Winter mean air temperature profiles over the SH region from the ERA-interim for the period 1989–1993 and 2005–2009.

AO and the SH (Figure 5a). In the latter part of the 20th century, the AO index showed a clear tendency toward a more positive phase, which could account for a considerable amount of the Northern Hemisphere surface temperature variation during the 20th century [*Thompson and Wallace*, 1998]. However, the tendency abruptly ceased in the mid 1990s, and the AO has mainly been in a near-neutral or negative phase since then [*Overland and Wang*, 2005]. Figure 5b compares the observed (HadSLP2) variation of the SHI which is linearly associated with the AO index (taking the SHI from the monthly AO-regressed SLP anomalies). The AO-related SHI fairly well matches with the observed SHI fluctuations, including both the decreasing and recovering SHI trends in recent decades. More physical explanation on the impact of AO change on the SHI, particularly on the recent SH recovering, is as follows. The negative trend of AO represents the weakening of tropospheric westerlies and anticyclonic pressure anomalies over the Arctic and high-latitudes. These conditions might allow more cold air from the Arctic to move south, resulting in temperature cooling over the northern Eurasian continent [*Overland and Wang*, 2010]. Also decreasing cloudiness associated with high-pressure anomalies over the Arctic and high-latitudes may also have a cooling effect. Therefore the building-up of cold-air mass in high-pressure center of SH can be reinforced by the negative AO trend. One thing to note is that such dynamical linkage between the AO and SH has been strengthened in the recent two decades. According to an examination of systematic spatial changes in NH atmospheric circulations by *Zhang et al.* [2008], since the early 1990s, there has been a radical shift in the spatial pattern of the AO where the negative center of action over the Arctic region has moved southeastward to the northern Eurasian continent. This shifted AO pattern displays a more direct linkage between the large-scale circulation (i.e., AO) and SH as the shifted Arctic center mostly covers the northern part of central SH region.

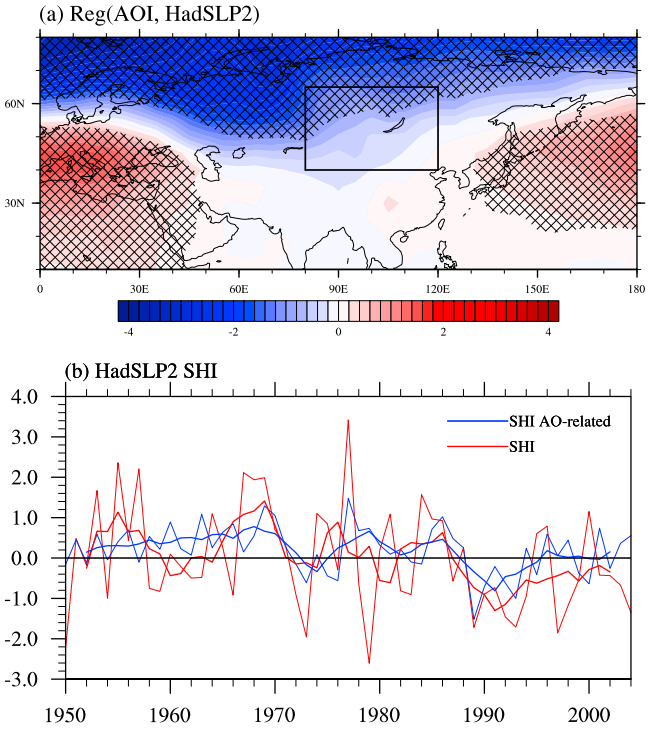

Figure 5. (a) Spatial pattern of the regressed monthly AO index (taken at http://www.cpc.noaa.gov/products/precip/CWlink/daily_ao_index/ao.shtml) to the monthly SLP anomalies for winter [hPa]. Areas with linear relationships between the two exceeding the 99% confidence level are marked with hatching. The box indicates the central region of the SH (40–65°). (b) The observed (HadSLP2) time series of the winter SHI, and the SHI associated with the AO-related SLP variation (by projecting the monthly AO index on the regression pattern in Figure 5a, monthly SLP anomalies linearly related with AO index are estimated. Then the area averaged SLP over the SH region, the AO-related SHI, is estimated).

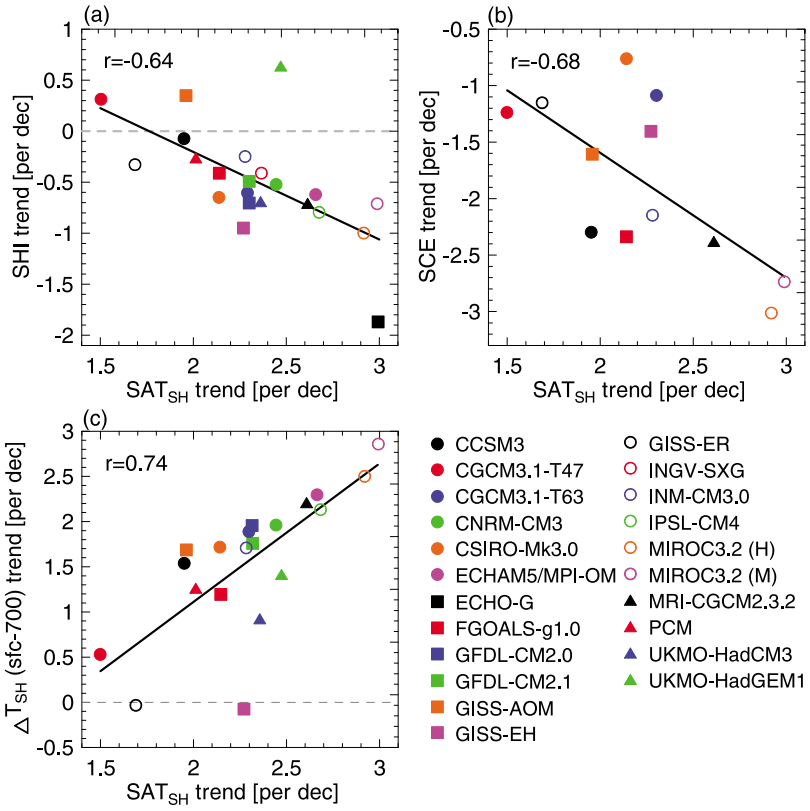

Figure 6. Projected relationships among linear trends in SHI, SAT over the SH center (SATSH), Eurasian snow cover, and ΔTSH (sfc–700) (air temperature difference between surface and 700 hPa over SH center) for the 21st century from the CMIP3 experiments under the A1B scenario. Represented as (a) SATSH versus SHI, (b) SATSH versus Eurasian snow cover extent (SCE), and (c) SATSH versus ΔTSH(sfc–700) trend. Full names and details of the 22 GCMs are available online at http://www-pcmdi.llnl.gov/ipcc/model_documentation/ipcc_model_documentation.php.

3.3. Future Projections of SHI by GCMs

[15] The SHI variations simulated by GCMs for the 20th and 21st century from 22 GCMs under 20C3M and A1B scenarios in the CMIP3 are examined (Figure 1b). The dramatic change in the SHI over the recent decades is not reproduced by any of the individual GCM simulations (figure not shown). In the ensemble mean of the GCMs (Figure 1b), the only notable feature is a steady decreasing trend in the SHI from the late 20th century throughout the 21st century, leading to a decrease of about 22% in SHI at the end of 21st century compared to the 1958–1980 average.

[16] Although we would not expect that the GCMs realistically simulate such a transient change in a specific region of interest, it could be intriguing to examine the suggested relationship between SHI and snow cover change simulated by the GCMs. We have briefly examined this with cross-comparisons of the simulated SAT trend in the SH center versus SHI, Eurasian SCE, and lower tropospheric stability (defined as an air temperature difference between the surface and 700 hPa over the SH center) for the 21st century estimated from the suite of GCM simulations (Figure 6).

[17] A majority of the GCMs (19 out of 22) indicate negative SHI trends for 21st century, where GCMs with a larger surface warming trend tend to show a stronger weakening trend of SHI (Figure 6a). All 10 GCMs which provide snow cover data indicate negative trends in Eurasian SCE. The rate also tends to be proportional to the magnitude of the simulated SAT warming (Figure 6b, the result with late fall SCE is almost similar to this), suggesting that the snow-albedo feedback is effectively working in the GCM simulations. Therefore, the largest warming is found at the near surface level for all 22 GCMs (figure not shown), and consequently the trend in the atmospheric stability is highly proportional to the SAT trend (Figure 6c). This indicates that a GCM simulating a larger surface warming tends to have a larger weakening of the atmospheric stability, which further fosters a larger SHI weakening.

[18] The results imply that the SHI simulated by GCMs is highly sensitive to the change in the Eurasian snow cover. Thus, the GCMs' inability to capture the recent SHI recovery is highly associated with their misrepresentation of the recent trend in the Eurasian snow cover and the associated feedback effect on SATs. Consequently, this suggests that we need to be cautious about the GCMs' ability to simulate Eurasian snow cover variability when assessing predictions of future changes in the SHI.

4. Summary and Discussion

[19] The present study notes a distinct interdecadal variation of SHI in the last few decades, emphasizing Eurasian

snow cover change as a primary influence. Confirming a pronounced declining trend of the SHI from the late 1960s to the early 1990s, we show that the declining trend was sharply replaced by a steep recovering trend in recent two decades. It is suggested that an increase in Eurasian snow cover over the last two decades and associated near-surface cooling over the SH central region have contributed the strengthening of the SHI. However, this feature has not been successfully captured by the GCM simulations used for the IPCC AR4. Future projections of SAT and SHI by GCMs are found to be very sensitive to simulated Eurasian snow cover, which keeps continuously decreasing in the future. As a result, GCMs predict a continuous decrease in SHI throughout the 21st century.

[20] Despite its suggested importance, the cause of the recent Eurasian snow cover increase has not been investigated in the present study. We assume that when the available atmospheric moisture content increases with a temperature increase it may promote the chance of precipitation as snow in the cold regions where temperatures are below freezing. However, this interpretation may not be applicable to the declining snow cover trend before the 1990s, which is interpreted to be the result of more snow melting because of warmer temperatures. As the response of snow cover to climate change is highly nonlinear in its spatial pattern and extent [*Groisman et al.*, 2006; *Hardiman et al.*, 2008], it is necessary to carefully examine changes in moisture and energy fluxes over northern Eurasia accompanying the recent climate change. We speculate that the marked Arctic sea-ice melting [*Comiso et al.*, 2008; *Stroeve et al.*, 2008] could exert remote influences on the Eurasian snow cover, by affecting the moisture and energy fluxes in the Arctic through the northernmost Eurasian continent. In fact, a GCM experiment with a reduced Arctic sea-ice cover indicated an increased southward moisture transport from the less ice-covered Arctic Ocean leading to an increase of the snow cover, particularly in the central and eastern part of northern Eurasia [*Deser et al.*, 2010]. In our further work, we plan to investigate the influence of accelerated arctic sea-ice melting on the change in recent snow cover over Siberia in the last decades through a GCM simulation.

[21] **Acknowledgments.** Jee-Hoon Jeong acknowledges the supports from the center of Earth System Science at the University of Gothenburg (TELLUS) and APEC Climate Center (APCC) international research project. Hans Linderholm was supported by Sida project SWE-2009-245. Seong-Joong Kim was supported by the project "Reconstruction and observation of components for the Southern Annular Mode (SAM) to investigate the cause of climate change at West Antarctica (PE11010)" of Korea Polar Research Institute. We appreciate Rosanne D'Arrigo who kindly supplied tree ring reconstructed SHI data.

References

Allan, R., and T. Ansell (2006), A new globally complete monthly historical gridded mean sea level pressure dataset (HadSLP2), 1850–2004, *J. Clim.*, *19*(22), 5816–5842, doi:10.1175/JCLI3937.1.

Armstrong, R. L., and M. J. Brodzik (2005), Northern Hemisphere EASE-Grid Weekly Snow Cover and Sea Ice Extent Version 3, http://nsidc.org/data/nsidc-0046.html, Natl. Snow and Ice Data Cent., Boulder, Colo.

Boyle, J. S., and T. J. Chen (1987), Synoptic aspects of the wintertime east Asian monsoon, in *Monsoon Meteorology*, edited by C. P. Chang and T. N. Krishnamurthy, pp. 125–160, Oxford Univ. Press, Oxford, U. K.

Brohan, P., J. J. Kennedy, I. Harris, S. F. B. Tett, and P. D. Jones (2006), Uncertainty estimates in regional and global observed temperature changes: A new data set from 1850, *J. Geophys. Res.*, *111*, D12106, doi:10.1029/2005JD006548.

Chang, C. P., K. M. Lau, and H. Hendon (2006), The Asian winter monsoon, in *The Asian Monsoon*, edited by B. Wang, pp. 89–127, Springer Praxis, New York, doi:10.1007/3-540-37722-0_3.

Cohen, J., and D. Entekhabi (1999), Eurasian snow cover variability and Northern Hemisphere climate predictability, *Geophys. Res. Lett.*, *26*(3), 345–348, doi:10.1029/1998GL900321.

Cohen, J., and C. Fletcher (2007), Improved skill of Northern Hemisphere winter surface temperature predictions based on land-atmosphere fall anomalies, *J. Clim.*, *20*(16), 4118–4132, doi:10.1175/JCLI4241.1.

Cohen, J., K. Saito, and D. Entekhabi (2001), The role of the Siberian High in Northern Hemisphere climate variability, *Geophys. Res. Lett.*, *28*(2), 299–302, doi:10.1029/2000GL011927.

Cohen, J., M. Barlow, P. J. Kushner, and K. Saito (2007), Stratosphere-troposphere coupling and links with Eurasian land surface variability, *J. Clim.*, *20*(21), 5335–5343, doi:10.1175/2007JCLI1725.1.

Cohen, J., M. Barlow, and K. Saito (2009), Decadal fluctuations in planetary wave forcing modulate global warming in late boreal winter, *J. Clim.*, *22*(16), 4418–4426, doi:10.1175/2009JCLI2931.1.

Cohen, J., J. Foster, M. Barlow, K. Saito, and J. Jones (2010), Winter 2009–2010: A case study of an extreme Arctic Oscillation event, *Geophys. Res. Lett.*, *37*, L17707, doi:10.1029/2010GL044256.

Comiso, J. C., C. L. Parkinson, R. Gersten, and L. Stock (2008), Accelerated decline in the Arctic Sea ice cover, *Geophys. Res. Lett.*, *35*, L01703, doi:10.1029/2007GL031972.

D'Arrigo, R., G. Jacoby, R. Wilson, and F. Panagiotopoulos (2005), A reconstructed Siberian High index since A. D. 1599 from Eurasian and North American tree rings, *Geophys. Res. Lett.*, *32*, L05705, doi:10.1029/2004GL022271.

Dee, D. P., and S. Uppala (2009), Variational bias correction of satellite radiance data in the ERA-Interim reanalysis, *Q. J. R. Meteorol. Soc.*, *135*(644), 1830–1841, doi:10.1002/qj.493.

Deser, C., R. Tomas, M. Alexander, and D. Lawrence (2010), The seasonal atmospheric response to projected Arctic sea ice loss in the late twenty-first century, *J. Clim.*, *23*(2), 333–351, doi:10.1175/2009JCLI3053.1.

Ding, Y. H. (1990), Buildup, air-mass transformation and propagation of Siberian High and its relations to cold surge in East Asia, *Meteorol. Atmos. Phys.*, *44*(1–4), 281–292.

Esper, J., E. R. Cook, and F. H. Schweingruber (2002), Low-frequency signals in long tree-ring chronologies for reconstructing past temperature variability, *Science*, *295*(5563), 2250–2253, doi:10.1126/science.1066208.

Fletcher, C. G., S. C. Hardiman, P. J. Kushner, and J. Cohen (2009), The dynamical response to snow cover perturbations in a large ensemble of atmospheric GCM integrations, *J. Clim.*, *22*(5), 1208–1222, doi:10.1175/2008JCLI2505.1.

Gillett, N. P., F. W. Zwiers, A. J. Weaver, and P. A. Stott (2003), Detection of human influence on sea-level pressure, *Nature*, *422*(6929), 292–294, doi:10.1038/nature01487.

Gong, D. Y., and C. H. Ho (2002), The Siberian High and climate change over middle to high latitude Asia, *Theor. Appl. Climatol.*, *72*(1–2), 1–9, doi:10.1007/s007040200008.

Groisman, P. Y., R. W. Knight, V. N. Razuvaev, O. N. Bulygina, and T. R. Karl (2006), State of the ground: Climatology and changes during the past 69 years over northern Eurasia for a rarely used measure of snow cover and frozen land, *J. Clim.*, *19*(19), 4933–4955, doi:10.1175/JCLI3925.1.

Hardiman, S. C., P. J. Kushner, and J. Cohen (2008), Investigating the ability of general circulation models to capture the effects of Eurasian snow cover on winter climate, *J. Geophys. Res.*, *113*, D21123, doi:10.1029/2008JD010623.

Intergovernmental Panel on Climate Change (2007), *Climate Change 2007: The Physical Science Basis: Contribution of Working Group I to the Fourth Assessment Report of the Intergovernmental Panel on Climate Change*, edited by S. Solomon et al., 996 pp., Cambridge Univ. Press, Cambridge, U. K.

Jones, C. G., P. Samuelsson, and E. Kjellström (2011), Regional climate modelling at Rossby Centre, *Tellus, Ser. A*, *63*, 1–3.

Kalnay, E., et al. (1996), The NCEP/NCAR 40-year reanalysis project, *Bull. Am. Meteorol. Soc.*, *77*(3), 437–471, doi:10.1175/1520-0477(1996)077<0437:TNYRP>2.0.CO;2.

Kanamitsu, M., W. Ebisuzaki, J. Woollen, S. K. Yang, J. J. Hnilo, M. Fiorino, and G. L. Potter (2002), NCEP-DOE AMIP-II reanalysis (R-2), *Bull. Am. Meteorol. Soc.*, *83*(11), 1631–1643, doi:10.1175/BAMS-83-11-1631.

Liu, Y., J. R. Key, and X. Wang (2009), Influence of changes in sea ice concentration and cloud cover on recent Arctic surface temperature trends, *Geophys. Res. Lett.*, *36*, L20710, doi:10.1029/2009GL040708.

Meehl, G. A., C. Covey, T. Delworth, M. Latif, B. McAvaney, J. F. B. Mitchell, R. J. Stouffer, and K. E. Taylor (2007), The WCRP CMIP3

multimodel dataset: A new era in climate change research, *Bull. Am. Meteorol. Soc.*, *88*(9), 1383–1394, doi:10.1175/BAMS-88-9-1383.
Onogi, K., et al. (2007), The JRA-25 reanalysis, *J. Meteorol. Soc. Jpn.*, *85*(3), 369–432, doi:10.2151/jmsj.85.369.
Orsolini, Y. J., and N. G. Kvamstø (2009), Role of Eurasian snow cover in wintertime circulation: Decadal simulations forced with satellite observations, *J. Geophys. Res.*, *114*, D19108, doi:10.1029/2009JD012253.
Overland, J. E., and M. Wang (2005), The Arctic climate paradox: The recent decrease of the Arctic Oscillation, *Geophys. Res. Lett.*, *32*, L06701, doi:10.1029/2004GL021752.
Overland, J. E., and M. Wang (2010), Large-scale atmospheric circulation changes are associated with the recent loss of Arctic sea ice, *Tellus, Ser. A*, *62*(1), 1–9, doi:10.1111/j.1600-0870.2009.00421.x.
Panagiotopoulos, F., M. Shahgedanova, A. Hannachi, and D. B. Stephenson (2005), Observed trends and teleconnections of the Siberian High: A recently declining center of action, *J. Clim.*, *18*(9), 1411–1422, doi:10.1175/JCLI3352.1.
Robinson, D. A., K. F. Dewey, and R. R. Heim (1993), Global snow cover monitoring: An update, *Bull. Am. Meteorol. Soc.*, *74*(9), 1689–1696, doi:10.1175/1520-0477(1993)074<1689:GSCMAU>2.0.CO;2.
Sahsamanoglou, H. S., T. J. Makrogiannis, and P. P. Kallimopoulos (1991), Some aspects of the basic characteristics of the Siberian anticyclone, *Int. J. Climatol.*, *11*(8), 827–839, doi:10.1002/joc.3370110803.
Saito, K., J. Cohen, and D. Entekhabi (2001), Evolution of atmospheric response to early season Eurasian snow cover anomalies, *Mon. Weather Rev.*, *129*(11), 2746–2760, doi:10.1175/1520-0493(2001)129<2746:EOARTE>2.0.CO;2.
Stroeve, J., M. Serreze, S. Drobot, S. Gearheard, M. Holland, J. Maslanik, W. Meier, and T. Scambos (2008), Arctic sea ice extent plummets in 2007, *Eos Trans. AGU*, *89*(2), 13, doi:10.1029/2008EO020001.
Thompson, D. W. J., and J. M. Wallace (1998), The Arctic Oscillation signature in the wintertime geopotential height and temperature fields, *Geophys. Res. Lett.*, *25*(9), 1297–1300, doi:10.1029/98GL00950.
Trenberth, K. E., and D. A. Paolino (1980), The Northern Hemisphere sea-level pressure dataset: Trends, errors and discontinuities, *Mon. Weather Rev.*, *108*(7), 855–872, doi:10.1175/1520-0493(1980)108<0855:TNHSLP>2.0.CO;2.
Uppala, S. M., et al. (2005), The ERA-40 re-analysis, *Q. J. R. Meteorol. Soc.*, *131*, 2961–3012, doi:10.1256/qj.04.176.
Wang, B. (2006), *The Asian Monsoon*, 787 pp., Springer, Berlin.
Wu, B. Y., and J. Wang (2002), Winter Arctic Oscillation, Siberian High and East Asian winter monsoon, *Geophys. Res. Lett.*, *29*(19), 1897, doi:10.1029/2002GL015373.
Wu, R., J. L. Kinter, and B. P. Kirtman (2005), Discrepancy of interdecadal changes in the Asian region among the NCEP-NCAR reanalysis, objective analyses, and observations, *J. Clim.*, *18*(15), 3048–3067, doi:10.1175/JCLI3465.1.
Zhang, X., A. Sorteberg, J. Zhang, R. Gerdes, and J. C. Comiso (2008), Recent radical shifts of atmospheric circulations and rapid changes in Arctic climate system, *Geophys. Res. Lett.*, *35*, L22701, doi:10.1029/2008GL035607.
Zhang, Y., K. R. Sperber, and J. S. Boyle (1997), Climatology and interannual variation of the East Asian winter monsoon: Results from the 1979–95 NCEP/NCAR reanalysis, *Mon. Weather Rev.*, *125*(10), 2605–2619, doi:10.1175/1520-0493(1997)125<2605:CAIVOT>2.0.CO;2.

D. Chen, J.-H. Jeong, H. W. Linderholm, and T. Ou, Department of Earth Sciences, University of Gothenburg, Box 460, SE-405 30, Gothenburg, Sweden. (jee-hoon.jeong@gvc.gu.se)
B.-M. Kim and S.-J. Kim, Korea Polar Research Institute, Box 32, 406-840, Incheon, South Korea.
J.-S. Kug, Korea Ocean Research and Development Institute, Box 29, 425-600, Ansan, South Korea.